Growth and Self-Assembly of Ultrathin Au Nanowires into Expanded Hexagonal Superlattice Studied by in Situ SAXS

Anais Loubat, M. Impéror-Clerc, B. Pansu, F. Meneau, Bertrand Raquet, G. Viau, Lise-Marie Lacroix

Growth and Self Assembly of Ultrathin Au Nanowires into Expanded Hexagonal Superlattice Studied by in situ SAXS

*Anaïs Loubat,[a,b] Marianne Impéror-Clerc,[c] Brigitte Pansu,[c] Florian Meneau,[d] Bertrand Raquet,[b] Guillaume Viau[a] and Lise-Marie Lacroix.[a]**

a. Université de Toulouse, INSA, UPS, LPCNO (Laboratoire de Physique et Chimie des Nano-Objets), F-31077 Toulouse, France; CNRS; UMR 5215 ; LPCNO, F-31077 Toulouse, France lmlacroi@insa-toulouse.fr; phone +33561559652, fax +33561559697

b. Laboratoire National des Champs Magnétiques Intenses, CNRS-INSA-UJF-UPS, UPR3228; 143 Avenue de Rangueil, F-31400 Toulouse, France

c. Laboratoire de Physique de Solides, UMR 8502, Bat. 510, Université Paris-Sud, F-91405 Orsay, France

d. SWING, Synchrotron Soleil, BP 48, F-91192 Gif-sur-Yvette, France

KEYWORDS. 1D growth. In situ SAXS. Metallic nanowires. Van der Waals forces.

We report the self-assembly of gold nanowires into hexagonal superlattices in liquid phase followed by in-situ Small Angle X Ray Scattering and give new insights on their growth mechanism. The unprecedented large interwire distance of 8 nm strongly suggests the stabilization of the ultrathin gold nanowires by a ligand's double layer composed of oleylamine and oleylammonium chloride. The one-dimensional growth is discussed, opening perspectives towards the control growth and self assemblies of metallic nanowires.

1. Introduction

In the last 20 years, improvement in liquid-phase synthesis opened the way towards controlled nanoparticles with adjustable size and very narrow size dispersion ($\sigma < 10\%$).[1] Though leading to a fine tuning of the physical properties, the shape control of the nanoparticles is still under investigation. Anisotropic metallic nanoparticles, which exhibit modified plasmonic resonance or stable magnetization compared to their spherical counterparts,[2,3] arisen from non isotropic growth processes.[4] Au nanorods, prepared in aqueous media, were one of the most studied systems, due to the inertness of the materials and the multiple potential applications ranging from catalysis to biomedical applications.[5] However, several hypotheses are often invoked for such anisotropic growth: the nature of the seeds,[6] the preferential adsorption of surfactant on peculiar crystallographic faces,[7,8] or the existence of templates such as anisotropic micelles in which the growth occurred.[9]

Recently, ultrathin gold nanowires which exhibit a mean diameter in the range 1.5-2 nm and a micrometer length, attracted lots of interest due to their size homogeneity and their potential application as SERS probes,[10] lightweight foldable optoelectronics membranes,[11,12] or elastic coiled springs.[13] Their unique 1D feature confers them remarkable conductivity properties, such as quantum phenomena at room temperature, opening innovative routes in nanoelectronic.[14,15,16] Several strategies have been followed to synthesize these ultrathin nanowires. A gold salt ($HAuCl_4$ or AuCl) is reduced in pure oleylamine (OY)[17,18,19] or in a solution containing OY and an additional reducing agent.[10,20, 21] Self assembly of these ultrathin nanowires into very nice parallel arrays were observed on the TEM carbon grids,[10,17] or at water interface,[12] opening perspectives for artificially designed metamaterials.[22]

Though exiting, the reported synthesis did not univocally address the question of the growth mechanism, which is of prime interest to tune the size of the wires and thus, their physical properties. If the presence of OY was reported consensually as crucial for the 1D growth, Hadler et al. proposed an oriented attachment and ripening process of small seeds,[21] while Pazos-Perez et al. invoked a micellar growth.[19] Moreover, the driving force of the self assembly, which could be tuned to control the final metamaterial obtained, was not clearly evidenced. The potential pre assembly in solution, prior to solvent evaporation which is known as a strong driving force towards crystallization,[23,24] requires in-situ characterizations based on dynamic light scattering with conventional DLS[25,26] or Small Angle X-Ray Scattering (SAXS).

Real-time SAXS enables to address both the study of the growth mechanism of nanoparticles in liquid phase,[27] thanks to their specific scattering profile, and the in-situ crystallisation,[28] through additional Bragg peaks, similarly to conventional X-ray diffraction (XRD). Based on SAXS, we report here for the first time the formation of hexagonal superlattices of ultrathin gold nanowires in the liquid phase. The present in situ study gives new information about the driving force that originates the self assembly in solution. The unprecedented interwire distance of 8 nm suggests a bilayer stabilisation of Au nanowires leading to new perspective on their growth mechanism.

2. Experimental section

2.1 Au NWs synthesis

The ultrathin gold nanowires (NWs) were prepared following a synthesis adapted from B. Xing and co-workers.[10] Typically 10 mM solution of gold was prepared: 40 mg of $HAuCl_4,3H_2O$ were dissolved in a solution containing 1.32 mL oleylamine (OY, 400 mM, OY/Au = 40) in 6.60 mL of hexane. 2.05 mL of triisopropylsilane (TIPS, 1M, TIPS/Au = 100) were added to initiate the gold reduction. Though the exact mechanism still unclear, TIPS acts as a strong reducing agent, fastening

the reaction from several days to few hours. The solution was then kept undisturbed at 40°C for few hours. Magnetic stirring did not drastically change the morphology of the final nanowires as shown in figure S1.

The effect of OY concentration on the growth of Au NWs was studied following the same procedure. OY was varied from 20 mM to 2000 mM, corresponding to 66 µL and 6.60mL respectively. The volume of hexane was adjusted from 7.85 mL to 0 mL in order to keep a gold concentration of 10 mM.

2.2 Characterization

A kinetic study of the growth mechanism of ultrathin gold nanowires coupling ex situ (TEM) and in situ (SAXS) was performed. The 10 mL solution was splitted into a 15 mL- glass vial and a sealed glass capillary tube for the SAXS analysis. Both conditioners were placed at 40 °C during 30 h. Aliquots were taken regularly with time to perform an ex situ TEM study of the evolution of the nanoparticles. To limit artefacts, aliquots were directly deposited, without any dilution or purification, on copper grids. TEM images were obtained with a JEOL-1011F microscope, operating at 100kV.

In situ SAXS measurements were performed on the same solution at 40 °C every 5 minutes for the first 3 hours and every 30 minutes from 3 to 30 h. The experiments were performed at the SWING beamline at the SOLEIL synchrotron using a monochromatic X-ray beam (10 keV). The reaction solution was introduced inside a glass capillary (1.5 mm in diameter) and the SAXS intensity was recorded on a CCD bi-dimensional detector placed inside a vacuum tube. The accessible q-range was between 6×10^{-3} and 0.6 $Å^{-1}$. For background subtraction, the capillary was measured first filled with the pure solvent (hexane) before introducing the reaction solution (inside the same capillary) to perform the in situ experiment. The SAXS intensities were experimentally normalized in absolute units (cm^{-1}) using water as a standard. This allowed quantifying the volume fractions in solution of

the spheres and the nanowires from the modeling results (supporting information for details), assuming a known value for the scattering contrast between gold and the solvent of 4420 ± 20 e/nm^3.

The final Au NWs were characterized by X-ray photoelectron spectroscopy (XPS) and solid state nuclear magnetic resonance (NMR) after a purification process. Briefly, 20 mL of absolute ethanol was added (Technical grade, VWR). Centrifugation at 4000 rpm during 5 min was performed. Au NWs were then redispersed in 5mL hexane and the precipitation repeated twice. X-ray photoelectron spectra were recorded using a Kratos Analytical Limited Axis ultra limited system fitted with a microfocused monochromatic Al Kα X-ray source (1486,6 eV, 12kV , 120W). The pass energy was set at 160 eV and 20 eV for the survey and the regions spectra respectively. Solid state NMR experiment of ^1H at magic angle spinning (MAS) was recorded on a Bruker Advance 400 spectrometer. Sample was packed into a 2.5 mm zirconia rotor and was spun at 24 kHz at room temperature.

3. Results and Discussion

3.1 Synthesis and characterization of Au NWs

We first tried to optimize the experimental condition for the synthesis of ultrathin Au NWs adapted from Xing et al.[10] We evidenced the strong influence of the OY concentration over the shape and size of the gold NPs. Solutions with [Au] = 10 mM, TIPS/Au = 100 and OY concentration varying from 20 to 2000 mM (OY/Au = 2 to 200) were prepared following the protocol previously described and placed at 40 °C for 24 h. Aliquots were taken after 5 h (Figure S2) and 24 h (Figure 1) directly deposited, without any dilution or purification, on copper grids for TEM characterization. For [OY] = 20 mM, only small spheres exhibiting a diameter ~ 1.5 nm were

observed. These spheres self organize on TEM grids, exhibiting an interparticle distance of ~ 2nm. For [OY] = 50 mM, very short rods were observed after 5 h but evolved towards spheres after 24 h (Figure 1b). Long wires were obtained and remained stable for oleylamine concentration in the range 100-1000 mM. At 2000 mM, the reaction was drastically slow down and after 12 h a white precipitate was observed. This precipitate could be identified as a lamellar phase composed of Au-Cl-oleylamine complexes, as previously described by Yang et coworkers.[17] After 24 h, Au nanowires were finally obtained concomitantly with ~ 8 nm spheres. Since the increase of oleylamine concentration favours the stabilization of Au NWs but decreases the reaction kinetics, a compromise should be found. In the following experiments, the oleylamine concentration was kept constant at 400 mM, in agreement with Xing et al.[10]

We then follow the evolution of ultrathin gold nanowires with time for [OY] = 400 mM. After 15 min, the TEM images showed two populations of spheres with mean diameter of 1.5 nm and 5 nm, respectively. Short wires exhibiting a mean diameter of ~1.5 nm and a length of ~100 nm were also observed in a smaller proportion (Figure 2a). After 45 min, the proportion of nanowires increased, their diameter remained constant at ~1.5 nm while their length increased to ~500 nm (Figure 2b). No sign of size evolution could be detected for the spheres. After 3 h of reaction, parallel assemblies of micrometric-long ($l \geq 2$ µm) nanowires were mostly observed (Figure 2c). After 27 h of reaction (Figure 2d and S3), micrometric wires were still observed in coexistence with a reduced amount of the two populations of spheres (1.5 nm and 5 nm).

Final gold nanowires, precipitated from the hexane solution by addition of absolute ethanol, were characterized by XPS and solid state NMR. The main peaks observed in the XPS survey scan were Au 4f, C 1s, N 1s and Cl 2p peaks centered at ca. 84, 285, 400 and 198 eV, respectively (Figure S4). The Au $4f_{7/2}$ and $4f_{5/2}$ high resolution spectra were fitted with only one component corresponding to Au(0) peaks (Figure S5a). The N 1s high resolution spectrum revealed two peaks centered at 399 and 401 eV (Figure S5b) corresponding to the binding energy of N 1s of nitrogen atom in the

oleylamine (OY) and in the oleylammonium cation (referred to as OY^+), respectively.[29] The molar ratio $N(OY^+)/Cl$, determined from the integrated peak areas, was found very close to 1 as expected for an ammonium chloride. The molar ratio $N(OY)/N(OY^+)$ was also close to 1, indicating that the stabilization of purified Au nanowires was insured fairly equally by long chain amine and ammonium. The important presence of ammonium at the surface of Au NWs was confirmed by ^1H MAS NMR spectra of pure Au NWs (Figure S6). A signal at 7.7 ppm typical of NH_3^+ group of OY^+ could be observed. Thus, the ammonium chloride, resulting from the protonation of oleylamine by the gold precursor $HAuCl_4$, is strongly attached to the gold NWs.

3.3 SAXS growth study

We performed a kinetic study of the Au NWs growth obtained at 40°C from a 10mM gold solution with [OY] = 400 mM thanks to in-situ SAXS. The variation of the SAXS intensity during the first 150 minutes is reported in Figure 2a. The successive scattering curves were analyzed using the form factors of a mixture of polydisperse spheres and nanowires, in agreement with the simultaneous ex-situ TEM study (Figure 2). The SAXS profiles were nicely fitted (Inset Figure 3a) with the following adjustable parameters: diameter, polydispersity and volume fraction of gold spheres, diameter, polydispersity on the diameter and volume fraction of gold nanowires, and a small constant background contribution (details in supporting information).

At t = 0, the scattering profile fitting indicates only the presence of spheres, with a diameter of 1.7 nm and a large polydispersity (>30%). The larger spheres (5-10 nm) that appeared on the TEM grid (Figure 2a) were not detected with SAXS, revealing that their volume fraction in solution is very low compared to the ones of the small spheres. During the reaction, an additional scattering profile is observed, its intensity increased up to 80 min, following a q^{-1} law in the low-q region (Figure 3a), indicating the presence of more and more nanowires in solution. The diameter of the wires was

found constant at 1.7 nm with a polydispersity on the diameter distribution of only 2%, in good agreement with the TEM observations. The length of the gold nanowires was always too large to be estimated from the SAXS signals during the kinetics, and was fixed to an effective value of 100 nm for all fits, corresponding to the size resolution of the SAXS experimental setup.

The variation of the volume fraction of the 1.7 nm spheres and of the nanowires with time is plotted in Figure 3b. While only few variation of the sphere volume fraction was observed with time, the nanowires were actually detected by SAXS after 20 minutes in good agreement with the TEM observations. At 30 min, the sphere volume fraction reached a maximum and concomitantly, the rate of growth of the nanowires was the highest. Between 80 and 150 min the SAXS intensity hardly varied and was still fitted by a mixture of small spheres and ultrathin nanowires with nearly constant volume fractions. At 150 min these fractions were 5.3×10^{-5} and 1.8×10^{-5} for the wires and the spheres, respectively. The total volume fraction of 7.1×10^{-5} derived from SAXS at 150 min is in good agreement with the 10^{-4} value expected from a 10 mmol.L^{-1} solution, taking into account the overall precision of the calibration procedure of the SAXS intensity. Thus, we can conclude that after only 80 min of reaction i) essentially all Au atoms were contained either in the small spheres or in the nanowires and ii) that the proportion of the wires was large, corresponding to 73% of the initial Au introduced.

A similar kinetic study, coupling TEM (Figure S7) and SAXS (Figure S8), was performed at 25 °C. A growth following the same trend than at 40 °C was observed. Spheres were already present at t = 0 and their volume fraction remained fairly constant with time. Wires growth was slow down compared to the reaction at 40 °C. After 5h, the reaction was just completed as evidenced by the evolution of their respective volume fraction (Figure S9). Thus, as expected, reaction temperature has a drastic effect on the kinetic of the nanowires growth.

3.4 Self-assembly of Au NWs in liquid phase

Whereas no significant difference was detected on the TEM images between 3 and 28 h (Figure 2c-d), the SAXS profiles revealed four well resolved Bragg peaks, showing the presence of a long-range positional order between the nanowires after a few hours (Figure 4). The peak positions in the reciprocal space relative to the position of the first peak were $1 : \sqrt{3} : \sqrt{4} : \sqrt{7}$ characterizing a bi-dimensional hexagonal positional order in the plane normal to the wires. The lattice parameter of this hexagonal phase inferred from the peak positions was a = 9.7 nm ± 0.1 nm. The estimated domain size for the hexagonal phase derived from the width of the Bragg peaks was of 64 nm after 5 hours and 73 nm after 10 hours. Along with the increase in the intensity at small angles (characterized by a small oscillation near q = 0.015 $Å^{-1}$), this indicated that the hexagonal phase could grow in a morphology of elongated fibers, with a typical diameter of 70 nm. The isotropic SAXS signal on the 2D detector shows that these NW hexagonal organizations are randomly oriented in the capillary, evidencing an homogeneous nucleation of the self-assembly in liquid phase and not at the surface of the capillary glass tube. The experimental SAXS spectra could be completely fitted (for q values greater than 0.02 $Å^{-1}$) by a model curve including the hexagonal phase of nanowires (Bragg peaks) in coexistence with free nanowires in solution (details in supporting information). Interestingly, the form factor of the nanowires was equal for both contributions, with a diameter of d = 1.7 ± 0.05 nm, constant with time, indicating that the same type of nanowires was present in solution and inside the hexagonal phase. Quantitatively, the volume fraction of the free nanowires is found equal to 3.0×10^{-5} after 10 h, corresponding to a proportion of 60 % of nanowires, the other 40% being embedded within the hexagonal phase. Since the diameter d of the nanowires in the hexagonal phase was characterized, the interwire distance in the plane normal to the wires could be calculated as $(a - d)$ = 8 nm (Figure 5). The oleylamine chain length being 2.1 nm,[30] the interwire distance is then approximately 4 times the oleylamine length. The hexagonal phase could thus be described as a parallel assembly of 1.7 nm gold NWs coated

with an oleylamine/oleylammonium bilayer (Figure 5). The hypothesis of an hexagonal phase composed of Au NWs coated with a monolayer of ligands, and the vacancies filled with solvent, was at the present time discarded due to the large interwire distance inferred from TEM (from 5.2 to 6.1 nm, Figure S10), of course this assumption would only be validated by further characterizations, such as Small Angle Neutron Scattering (SANS).[31] After solvent evaporation, Au NWs coated by a monolayer would indeed lead to interwire distance in the range 2 – 4 nm, due to the partial interdigitation of alkyl chain upon solvent evaporation.[32]

The same kinetic study was performed by SAXS at 25°C (Figure S8). The hexagonal phase appeared after 6 h with a very similar lattice parameter, 9.9 ± 0.1 nm, taken into account the modification of the alkyl chain configuration with temperature.

Hexagonal phases of elongated objects in solution like DNA,[33] carbon nanotubes[34] or viruses,[35] and self assemblies of inorganic rods and wires were already characterized by SAXS[36] or on by TEM[20] but, to our knowledge, this is the first report of a well organized hexagonal phase in solution of metallic nanowires. Interestingly, our in situ study reveals that the nucleation of the hexagonal phase required an incubation time of nearly 3h after the formation of the NWs. In contrast, only a few seconds were needed for the self-assembly into super-lattices of 11.6 nm spherical Au nanoparticles at a similar volume fraction.[27] Such discrepancy can be explained by diffusion and orientation requirements prior to the nanowire organization and thus, a slower dynamics of the nucleation/growth in solution. The formation of nanoparticle super-lattices results from the delicate balance of attractive and repulsive forces.[37,38] In most cases, the driving force towards self-assembly is a strong Van der Waals attraction between the particles, which increases with nanoparticle polarizability and diameter. In such superlattices, interdigited ligands, leading to short interparticle distances are generally found.[39,40] In the case of water suspensions of charged anisotropic nanoparticles with strong electrostatic repulsion, entropic effects are inducing parallel organizations

with crystal liquid behaviour (Onsager theory).[41] Depletion attraction through excess of surfactants can also be at the origin of nanoparticles organizations.[37]

In the present case, the small diameter and the very large interwire distance insured by the ligand bilayer around each nanowire raise the question of the driving force of such self-assembly. Considering that the wire radius (R = 0.85 nm) is much smaller than the interaxial distance (a = 9.7 nm) and negligible compared to the wire length (L = 1000 nm), the Van der Waals energy between two parallel Au nanowires can be estimated according to Equation 1 (approximate expression valid for $R<<a<<L$).[42,43]

$$E_{VdW} = -\frac{3A}{8\pi}\frac{(\pi R)^4}{a^5}L \qquad \text{(Eq. 1)}$$

Due to comparable Hamaker constant of hexane and oleylamine,[44,45] the classical value of 75 kT usually considered for the Hamaker constant of gold nanoparticules in hexane,[46,47] is certainly a good approximation in our system, leading to E_{VdW} = -5.3 k_BT. This value has the same order of magnitude than in the case of spherical gold particle superlattices already reported.[38] The steric repulsion appears with ligands interdigitation, thus for interwire distances lower than the full extend of two oleylamine bilayers, i.e. below 4 × 2.1 nm = 8.4 nm. This steric repulsion insured by the bilayer at the surface of Au NWs could be responsible for the stabilisation of the hexagonal superlattices with an interwire distance as large as 8 nm.

3.5 Nanowire growth mechanism

Regarding the growth mechanism, we observed that the wire growth, at 40 °C or 25 °C, did not induce a diminution of the number of spheres, as revealed by the time evolution of the volume fraction of each type of particle (Figures 3b and S9). Such observation is in contradiction with a

growth mechanism based on oriented attachment of small spheres, where the wire growth would consume the initial 1.7 nm spheres. These small spheres appear mainly as side-product, but the slight decrease of their volume fraction after 30 min at 40 °C, concomitant with the highest nanowire growth rate, may stress their role as seeds.[48] The unprecedented large interwire distance in the hexagonal superlattice suggests a bilayer stabilisation of the Au nanowires. One can infer that this bilayer stabilisation may be also present at the surface of the free NWs, and not only inside the hexagonal superlattice. The XPS and NMR analysis showed that the stabilisation of purified Au nanowires is insured fairly equally by oleylamine and oleylammonium chloride. Such charged stabilisation reminds the CTAB bilayer, recently characterized by SANS,[31] at the surface of Au nanorods in water. We have also observed that the shape of the Au nanoparticles was strongly dependent of the oleylamine concentration initially introduced. This concentration effect reminds the phase diagram of surfactants like CTAB in aqueous media[44] and the critical micellar concentration associated with the transition from spherical to cylindrical micelles. All these observations suggest that a micellar growth mechanism drives the one-dimensional growth.

4. Conclusion

Owing to a in situ SAXS study, we were able to describe precisely for the first time the self assembly of ultrathin Au NWs into a hexagonal super-lattice in apolar solvent. This super-lattice exhibits a very large lattice parameter corresponding to an interwire distance of 8 nm. Such large value can be explained by the presence of a bilayer at the surface of each nanowires, composed of oleylamine and oleylammonium, as revealed by NMR and XPS. Along with the strong influence of the oleylamine concentration on the final shape of the Au nanoparticles, all these results suggest a micellar growth mechanism for the NWs. To have a deeper understanding of the supramolecular organisation of OY and OY^+/Cl^-, both at the surface of the nanowires and in the second layer, and

their impact on the growth of Au nanoparticles, coupled SANS and SAXS studies will be performed, while NMR, periodic-DFT and Monte-Carlo theoretical studies should give new insight on the chemical organisation of these micelles. The unprecedented hexagonal self assembly of micrometric long Au nanowires opens new perspectives for dedicated applications such as catalysis or electronic nanocontact.

Acknowledgments

Patrick Davidson (LPS, Orsay), Bruno Chaudret and Romuald Poteau (LPCNO, Toulouse) are warmly thanked for fruitful discussions. We thank Y. Coppel (LCC, Toulouse) for RMN measurements and G. Antorrena (INA, Saragossa) for XPS measurements. A. Robert is thanks for his help in the experimental section. Jan Skov Pedersen (University of Aahrus, Denmark) is specially thanked for his advices concerning the SAXS modelling. The authors acknowledge the financial support of the Midi-Pyrénées region, of the university of Toulouse, PRES, of the Labex NEXT, N° 11 LABX 075, of the French GDR Or-Nano and of the French network METSA.

Model for the SAXS intensity, XPS survey and high resolution scans and ^{1}H-MAS NMR spectrum of purified Au NWs. TEM and SAXS characterization of the kinetic study at 25 °C and the corresponding volume fraction evolution with time. This information is available free of charge via the Internet at http://pubs.acs.org/.

Figures

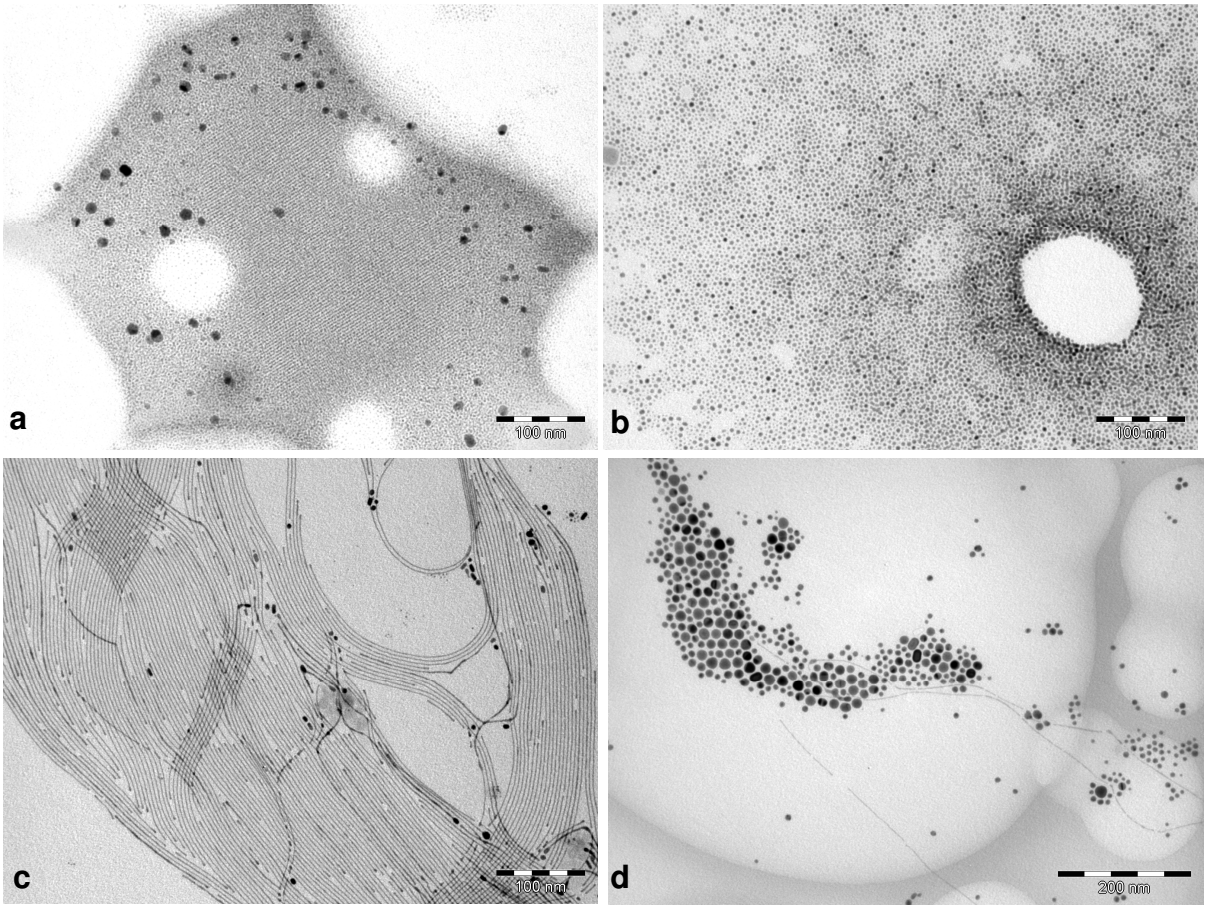

Figure 1

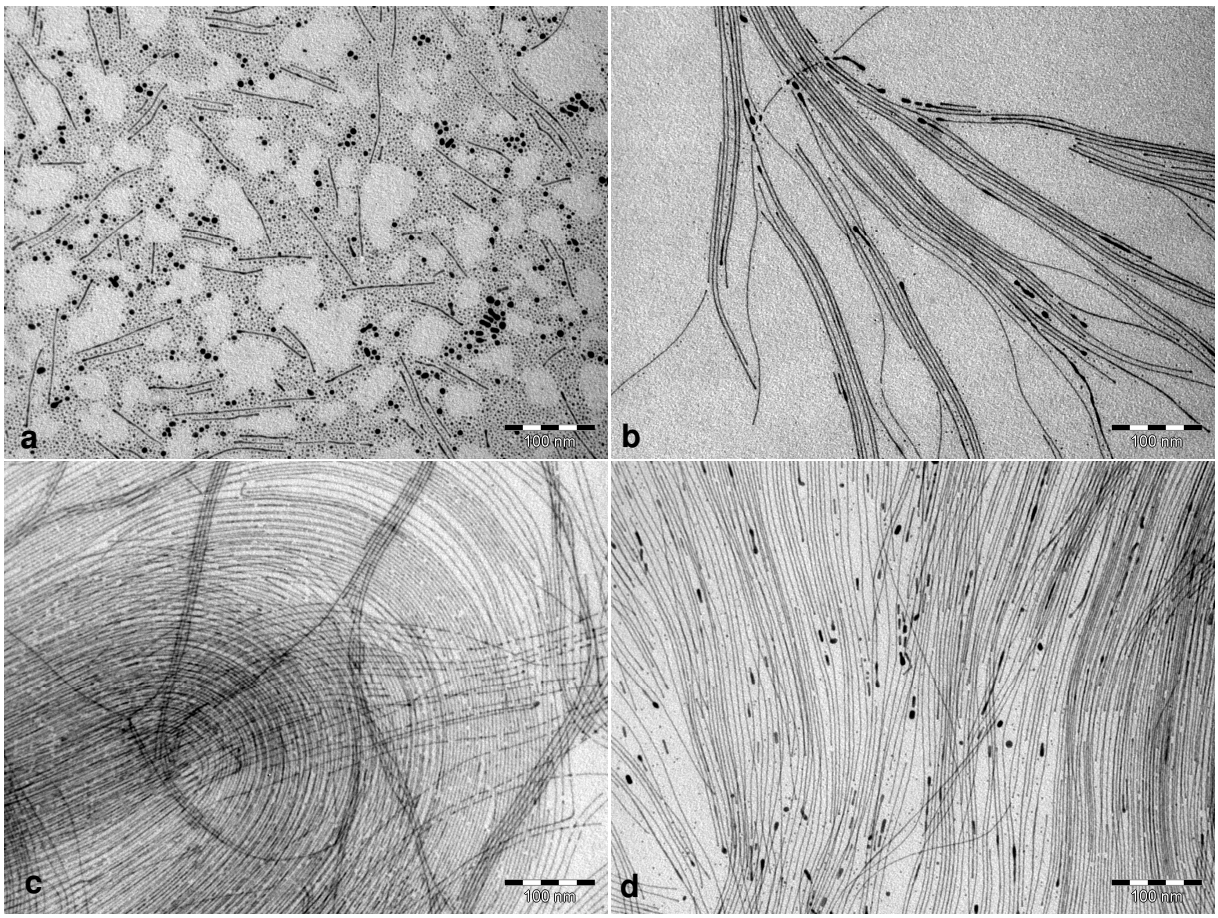

Figure 2

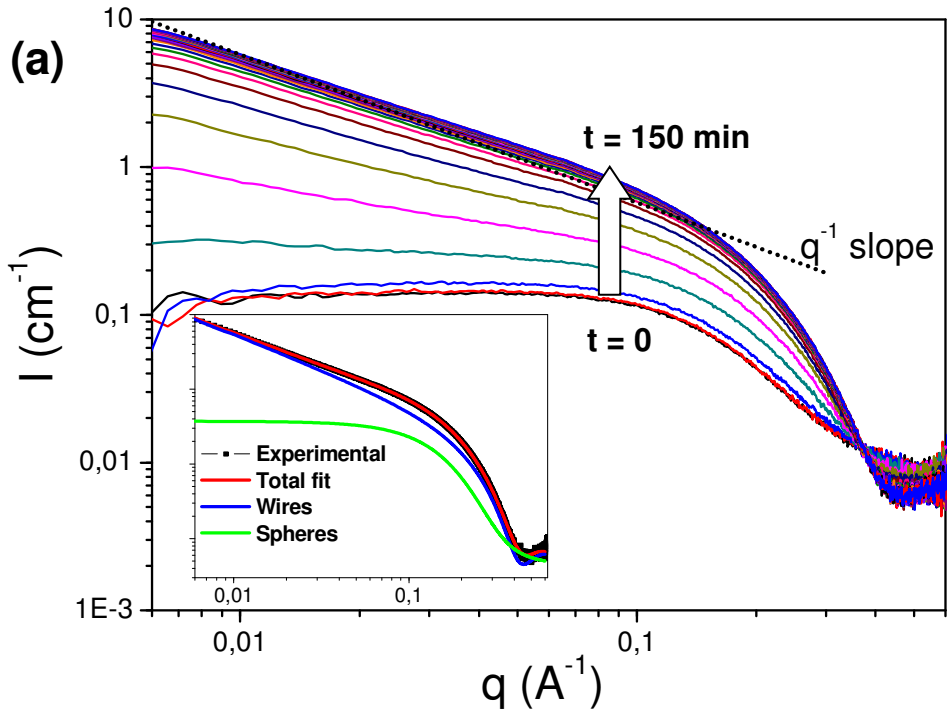
(a)
t = 150 min
t = 0
q^-1 slope
I (cm^-1)
q (A^-1)
Experimental
Total fit
Wires
Spheres

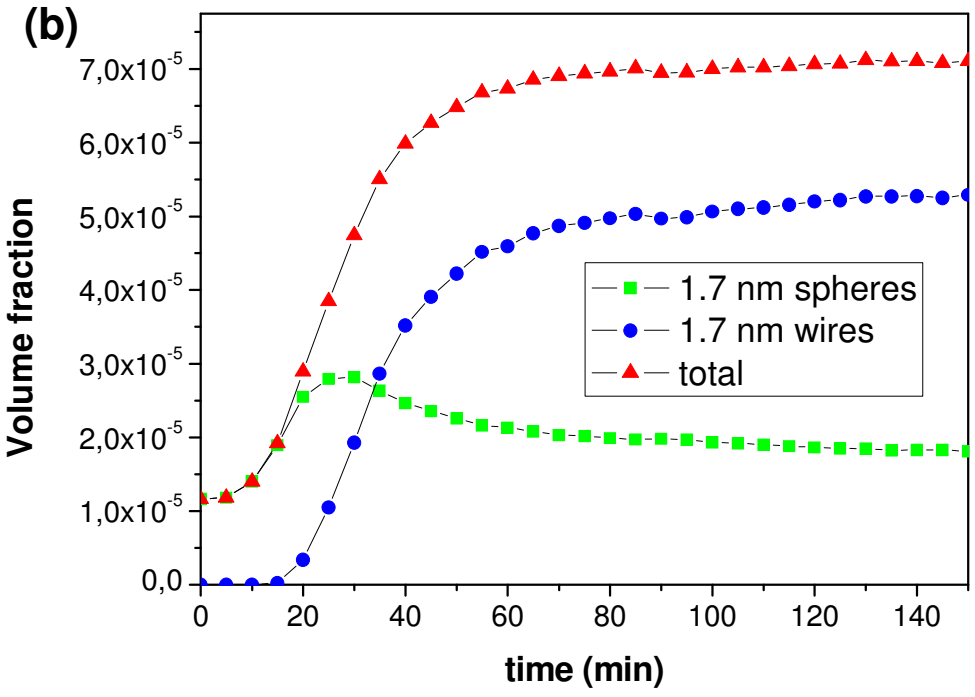
(b)
Volume fraction
time (min)
1.7 nm spheres
1.7 nm wires
total

Figure 3

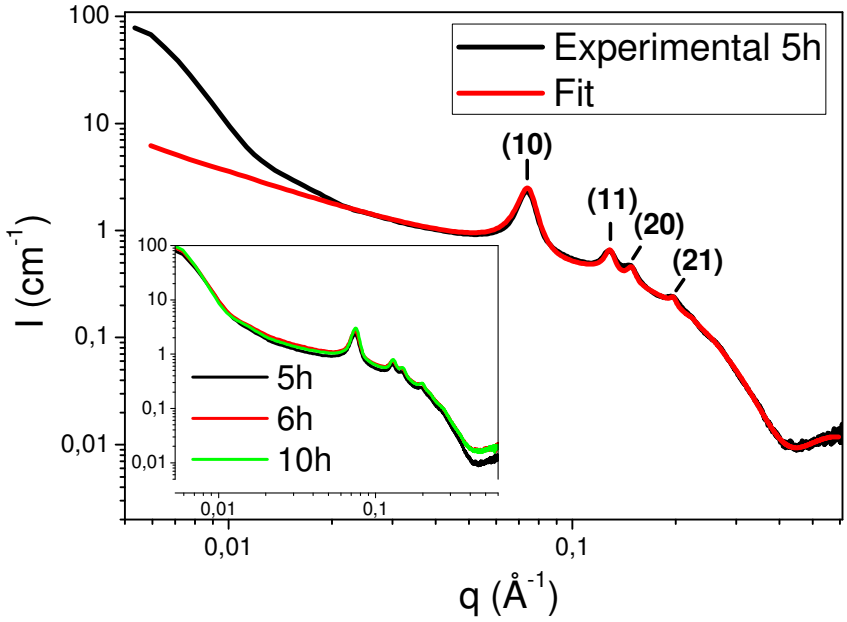
Experimental 5h
Fit
(10)
(11)
(20)
(21)
I (cm-1)
q (Å-1)
5h
6h
10h
100
10
1
0,1
0,01

Figure 4

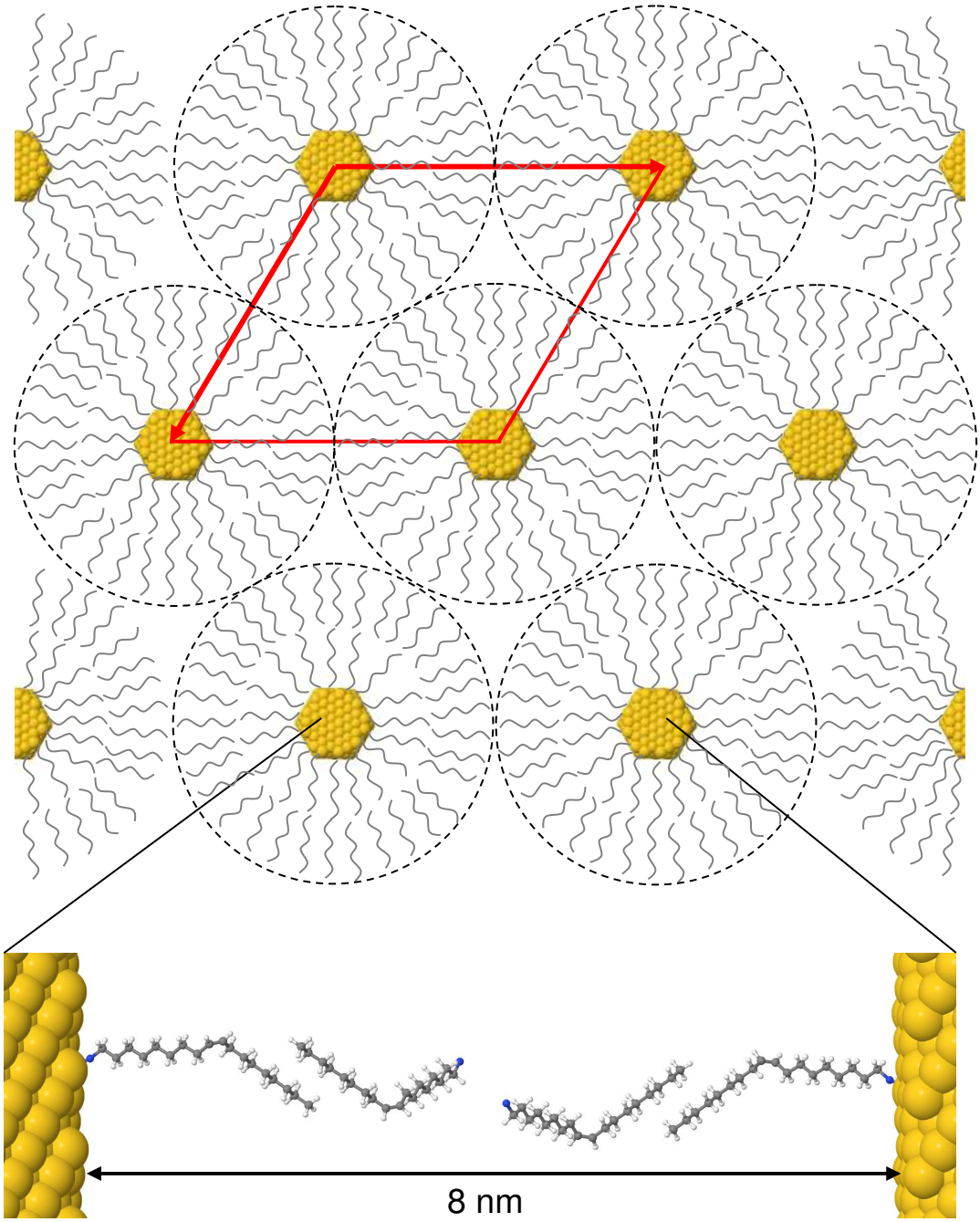

Figure 5

Figure legends

Figure 1: TEM image of Au NPs obtained after 24h at 40°C for TIPS/Au = 100 and [OY] = a) 20 ; b) 50 ; c) 100 and d) 2000 mM.

Figure 2: TEM images of Au nanoparticles obtained after a) 15 min, b) 45 min, c) 3 h and d) 27 h of reaction at 40 °C with [Au] 10 mM and [OY] = 400 mM

Figure 3: (a) Small angle X-ray scattering results measured at 40 °C every 5 min. *Inset*: Comparison with the experimental data at 150 min and the fitting curve as a sum of nanowires and spheres contributions. The q^{-1} slope in dashed line is a guide to the eyes; (b) Volume fraction calculated from the SAXS modelling at different times.

Figure 4: SAXS data of the hexagonal phase of nanowires at 5h, the fitting curve is a sum of the signal of the hexagonal phase (Bragg peaks) and of free nanowires remaining in solution. *Inset:* SAXS profile at different times.

Figure 5: Scheme of the hexagonal phase unit cell (arrows), we considered a 1.7 nm AuNW with an hexagonal cross-section, as suggested by A. Roy et al.[49]. The double layer around each nanowire is represented with a dashed circle and a possible arrangement of the four OY and/or OY^+ molecules is shown in the enlarged view. For simplification, only one type of isomers, corresponding to the fully extended molecules, is shown.

TOC

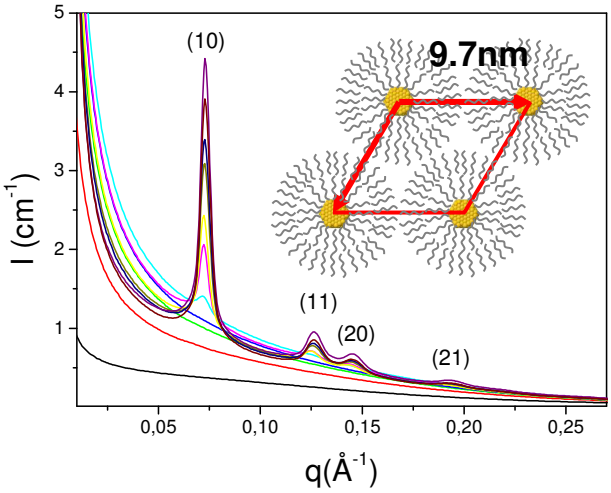

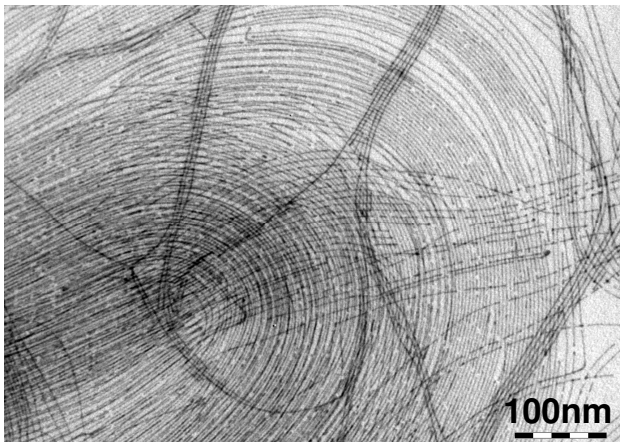

Notes and references

[1] Kwon, S. G.; Hyeon, T. Colloidal Chemical Synthesis and Formation Kinetics of Uniformly Sized Nanocrystals of Metals, Oxides, and Chalcogenides, *Acc. Chem. Res.*, **2008**, *41*, 1696-1709

[2] Pérez-Justea, J.; Pastoriza-Santosa, I.; Liz-Marzána, L. M.; Mulvaney, P. Gold nanorods: Synthesis, characterization and applications, *Coord. Chem. Rev.* **2005**, *249*, 1870-1901

[3] Lu, A.-H.; Salabas, E. L.; Schüth, F. Magnetic Nanoparticles: Synthesis, Protection, Functionalization, and Application, *Angew. Chem. Int. Ed.* **2007**, *46*, 1222 – 1244

[4] Sau, T. K.; Rogach, A. L. Nonspherical Noble Metal Nanoparticles: Colloid-Chemical Synthesis and Morphology Control, *Adv. Mater.* **2010**, *22*, 1781-1804

[5] Grzelczak, M.; Perez-Juste, J.; Mulvaney, P. A.; Liz-Marzan, L. M. Shape control in gold nanoparticle synthesis, *Chem. Soc. Rev.* **2008**, *37*, 1783-1791

[6] Lofton, C.; Sigmund, W. Mechanisms Controlling Crystal Habits of Gold and Silver Colloids *Adv. Funct. Mater.* **2005**, *15*, 1197-1208

[7] Murphy, C. J.; Thompson, L. B.; Alkilany, A. M.; Sisco, P. N.; Boulos, S. P.; Sivapalan, S. T.; Yang, J. A.; Chernak, D. J.; Huang, J. The Many Faces of Gold Nanorods, *J. Phys. Chem. Lett.* **2010**, *1*, 2867-2875

[8] Katz-Boon, H.; Rossouw, C. J.; Weyland, M.; Funston, A. M.; Mulvaney, P.; Etheridge, J. Three-Dimensional Morphology and Crystallography of Gold Nanorods, *Nano Lett.* **2011**, *11*, 273-278

[9] Gao, J.; Bender, C. M.; Murphy, C. J.; Dependence of the Gold Nanorod Aspect Ratio on the Nature of the Directing Surfactant in Aqueous Solution, *Langmuir*, **2003**, *19*, 9065-9070

[10] Feng, H.; Yang, Y.; You, Y.; Li, G.; Guo, J.; Yu, T.; Shen, Z.; Wu, T.; Xing, B. Simple and rapid synthesis of ultrathin gold nanowires, their self assembly and application in surface-enhanced Raman scattering, *Chem. Comm.*, **2009**, 1984

[11] Chen, Y.; Ouyang, Z.; Gu, M.; Cheng, W. Mechanically strong, optically transparent, giant metal superlattice nanomembranes from ultrathin gold nanowires, *Adv. Mater.* **2013**, *25*, 80-85

[12] Sanchez-Iglesias, A.; Rivas-Murias, B.; Grzelczak, M.; Perez-Juste, J.; Liz-Marzan, L. M.; Rivadulla, F.; Correa-Duarte, M. A. Highly transparent and conductive Films of densely aligned ultrathin Au nanowire monolayers, *Nano Lett.* **2012**, *12*, 6066-6070

[13] Xu, J.; Wang, H.; Liu, C.; Yang, Y.; Chen, T.; Wang, Y.; Wang, F.; Liu, X.; Xing, B.; Chen, H. Mechanical nanosprings : induced coiling and uncoiling of ulltrathin Au nanowires, *J. Am. Chem. Soc.* **2010**, *132*, 11920-11922

[14] Pud, S.; Kisner, A.; Heggen, M.; Belaineh, D.; Temirov, R.; Simon, U.; Offenhäusser, Mourzina, Y.; Vitusevich, Features of transport in ultrathin gold nanowire structures, *Small*, **2013**, *9*, 846-852

[15] Loubat, A.; Escoffier, W.; Lacroix, L.-M.; Viau, G.; Tan, R.; Carrey, J.; Warot-Fonrose B.; Raquet, B. Cotunneling transport in ultra-narow gold nanowire bundles, *Nano Res.* **2013***, 6*, 644-651

[16] Chandni , U.; Kundu ,P.; Kundu , S.; Ravishankar , S.; Ghosh A. Tunability of Electronic States in Ultrathin Gold Nanowires, *Adv. Mater.* **2013**, *25*, 2486–2491

[17] Huo, Z. ; Tsung, C.-K. ; Huang, W.; Zhang, X.; Yang, P. Sub-Two Nanometer Single Crystal Au Nanowires. *Nano Lett.,* **2008**, *8*, 2041-2044

[18] Lu, X.; Yavuz, M.S.; Tuan, H.-Y., Korgel, B.A.; Xia, Y. Ultrathin Gold Nanowires Can Be Obtained by Reducing Polymeric Strands of Oleylamine#AuCl complexes Formed by Aurophilic Interaction. *J. Am. Chem. Soc.* **2008**, *130*, 8900-8901

[19] Pazos-Pérez, N.; Baranov, D.; Irsen, S.; Hilgendorff, M.; Liz-Marzán, L.M.; Giersig, M. Synthesis of Flexible, Ultrathin Gold Nanowires in Organic Media. *Langmuir* **2008**, *24*, 9855-9860

[20] Kang, Y.; Ye, X.; Murray, C. B. Size- and shape-selective synthesis of metal nanocrystals and nanowires using CO as a reducing agent, *Angew. Chem. Int. Ed.* **2010**, *49*, 6156-6159

[21] Halder, A.; Ravishankar, N. Ultrafine Single-Crystalline Gold Nanowire Arrays by Oriented Attachment. *Adv. Mater.* **2007**, *19*, 1854-1858

[22] Nie, Z. ; Petukhova, A.; Kumacheva, E. Properties and emerging applications of self-assembled structures made from inorganic nanoparticles, *Nature Nanotech.*, **2009**, *5*, 15-25

[23] Rabani, E.; Reichman, D. R.; Geissler, P. L.; Brus, L. E. Drying-mediated self-assembly of nanoparticles, *Nature*,**2003**, *426*, 271-274

[24] Park, J.; Zheng, H.; Lee, W. C.; Geissler, P. L.; Rabani, E.; Alivisatos, A. P. Direct observation of nanoparticle superlattice formation by using liquid cell transmission electron microscopy, *ACS Nano*, **2012**, *6*, 2078-2085

[25] Miszta, K.; de Graaf, J.; Bertoni, G.; Dorfs, D.; Brescia, R.; Marras, S.; Ceseracciu, L.; Cingolani, R.; van Roij, R.; Dijkstra, M.; Manna, L. Hierarchical self-assembly of suspended branched colloidal nanocrystals into superlattice structures, *Nature Mater.* **2011**, *10*, 872-876

[26] Pagès, C. ; Coppel, Y. ; Kahn, M. L. ; Maisonnat, A. ; Chaudret, B. Self-assembly of ZnO nanocrystals in colloidal solutions. *Chem. Phys. Chem.* **2009**, *10*, 2334-2344

[27] Abécassis, B.; Testard, F.; Spalla, O. Gold Nanoparticles Superlattice Crystallization Probed *In Situ Phys. Rev. Lett.* **2008**, *100*, 115504

[28] Abécassis, B.; Testard, F.; Spalla, O.; Barboux, P. Probing in situ the nucleation and growth of gold nanoparticles by small-angle X-Ray scaterring. *Nano Lett.*, **2007**, *7*, 1723-1727

[29] Kumar, A. ; Mandal, S. ; Selvakannan, P. R. ; Pasricha, R. ; Mandale, A. B.; Sastry, M. Investigation into the interaction between surface-bound alkylamines and gold nanoparticles. *Langmuir*, **2003**, *19*, 6277-6282

[30] Mourdikoudis, S; Liz-Marzán, L.M. Oleylamine in Nanoparticle Synthesis. *Chem. Mater.* **2013**, *25*, 1465−1476

[31] Gomez-Grana, S. ; Hubert, F. ; Testard, F. ; Guerrero-Martinez, A. ; Grillo, I. ; Liz-Marzan, L. M. ; Spalla, O. Surfactant (Bi)layers on gold nanorods. *Langmuir* **2012**, *28*, 1453-1459

[32] Ge, G.; Brus, L. E. Fast surface diffusion of large disk-shaped nanocrystals aggregates. *Nano Lett.* **2001**, *1*, 219-222

[33] Livolant, F.; Levelut, A.M.; Doucet, J.; Benoit, J.P. The Highly Concentrated Liquid-Crystalline Phase of DNA is Columnar Hexagonal. *Nature* **1989**, *339*, 724-726

[34] Thess, A.; Lee, R.; Nikolaev, P.; Dai, H.; Petit, P.; Robert, J.; Xu, C.; Lee, Y. H.; Kim, S. G.; Rinzler, A. G. Colbert, D. T.; Scuseria, G. E.; Tománek, D.; Fischer, J. E.; Smalley, R. E. Crystalline Ropes of Metallic Carbon Nanotubes. *Science* **1996**, *273*, 483-487

[35] Grelet, E. Hexagonal Order in Crystalline and Columnar Phases of Hard Rods. *Phys. Rev. Lett.* **2008**, *100*, 168301.

[36] Hamon, C.; Postic, M.; Mazari, E.; Bizien, T.; Dupuis, C.; Even-Hernandez, P.; Jimenez, A.; Courbin, L.; Gosse, C. ; Artzner, F. ; Marchi-Artzner, V. Three-dimensional self-assembling of gold nanorods with controlled macroscopic shape and local smectic B order, *ACS Nano*, **2012**, *6*, 4137-4146

[37] Henzie, J. ; Grünwald, M. ; Widmer-Cooper, A. ; Geissler, P. L. ; Yang, P. Self-assembly of uniform polyhedral silver nanocrystals into densest packings and exotic superlattices. *Nature Mater.* **2012**, *11,* 131-137

[38] Goubet, N.; Richardi, J.; Albouy, P.-A.; Pileni, M.-P. Which forces control supercrystal nucleation in organic media? *Adv. Funct. Mater.* **2011**, *21*, 2693-2704

[39] Jiang, Z.; Lin, X.-M.; Sprung, M.; Narayanan, S.; Wang, J. Capturing the crystalline phase of two-dimensional nanocrystal superlattices in action. *Nano Lett.* **2010**, *10*, 799-803

[40] Lee, B. ; Podsiadlo, P. ; Rupich, S.; Talapin, D. V.; Rajh, T.; Schevchenko, E. Comparison of structural behaviour of nanocrystals in randomly packed films and long-range ordered superlattices by time-resolved small angle X-ray scattering. *J. Am. Chem. Soc.* **2009**, *131*, 16386-16388

[41] Lekkerkerker, H. N.W.; Vroege G. J. Liquid crystal phase transitions in suspensions of mineral colloids: new life from old roots, Phil Trans R Soc A **2013**, *371*, 20120263. http://dx.doi.org/10.1098/rsta.2012.0263..

[42] Parsegian, V. A. Van der Waals forces, Cambridge University Press, **2006.**

[43] Russel W.B., Saville D.A., Scholwalter W.R., Colloidal dispersions, Cambridge University Press, **1989**

[44] Israelachvili, J.N. Intermolecular and surface forces, 3rd ed. **2011**, Elsevier

[45] Jia, G.; Sitt, A.; Hitin, G. B.; Hadar, I.; Bekenstein, Y.; Amit, Y.; Popov, I.; Banin, U. Couples of colloidal semiconductor nanorods formed by self-limited assembly. *Nature Materials* **2014**, *13*,301–307

[46] Bargeman, D.; Van Voorst Vader, F. Van der Waals forces between immersed particles. *J. Electroanal. Chem.* **1972**, *37*, 45- 52

[47] Pansu, B; Lecchi, A; Constantin, D; Impéror-Clerc, M; Veber, M; Dozov, I. Insertion of Gold Nanoparticles in Fluid Mesophases: Size Filtering and Control of Interactions *J. Phys. Chem. C* **2011,** *115,* 17682–17687

[48] Azulai, D.; Cohen, E.; Markovich, G. Seed concentration control of metal nanowire diameter. *Nano Lett.* **2012**, *12*, 5552-5558

[49] Roy, A.; Pandey, T.; Ravishankar, N. & Singh, A. K. Single crystalline ultrathin gold nanowires: Promising nanoscale interconnects, *AIP Adv.* **2013,** *3***,** 032131